On nd Bonding in the Transition Metal Trimers: Comparison of Sc_3 and Y_3

Stephen P. Walch[a]

Eloret Institute
Sunnyvale,CA 94087

Abstract

CASSCF/CCI calculations are presented for the low-lying states of Y_3. Comparison of the wave functions for Y_3 and Sc_3 indicates substantial 4d-5p hybridization in Y_3, but little 3d-4p hybridization in Sc_3. The increased 4d-5p hybridization leads to stabilization of $4d\pi$ bonding with respect to $4d\sigma$ bonding for equilateral triangle Y_3, and also leads to 4d-5p bonding for linear geometries. These effects lead to a different ordering of states for equilateral triangle geometries and a smaller excitation energy to the linear configuration for Y_3 as compared to Sc_3.

[a]Mailing Address: NASA Ames Research Center, Moffett Field, CA 94035.

I. Introduction

Recently Knight, Woodward, VanZee, and Weltner[1] studied the ESR spectra of Sc_3 and Y_3 in rare gas matrices. The ESR spectrum for Sc_3 shows equivalent Sc atoms, which is consistent with an equilateral triangle ground state geometry. Calculations by Walch and Bauschlicher[2] find a $^2A_2''$ ground state for Sc_3 with the configuration:

$4sa_1'^2\ 4se'^4\ 3da_1'^2\ 3da_2''^1$

Here the $3da_1'$ and $3da_2''$ orbitals are 3d bonding orbitals derived from the atomic $3d\sigma$ and $3d\pi''$ orbitals, respectively. (The symmetry designations here are for D_{3h} symmetry and correspond to a σ axis along a line connecting a given atom with the center of the molecule.) From a comparison of the Sc_3 and Ca_3 potential curves, it is apparent that these 3d bonding orbitals contribute significantly to the bonding in this molecule. Also, some 4p involvement due to 4s-4p hybridization is found in the bonding in both Ca_3 and Sc_3. However, there is little admixture of 4p into the 3d like bonding orbitals.

For Y_3, the ESR spectrum shows only two equivalent Y atoms, which is consistent with a non - equilateral triangle structure (such as an obtuse angle bent molecule or a linear molecule). It was of interest to see if the calculations would show significant differences between the bonding in Sc_3 and Y_3, which could account for these differences which are observed experimentally. We find the major difference between these molecules is the increased importance of 5p-4d hybridization in the bonding orbitals of Y_3, relative to 4p-3d hybridization in Sc_3. This effect results in a different ordering of states for Y_3 as compared to Sc_3 and 5p-4d hybridization effects lead to a low-lying linear configuration for Y_3, while the calculations on Sc_3 clearly indicate an equilateral triangle ground state. In section II we briefly describe the calculational details. Section III describes the results obtained, and Section IV

presents the conclusions.

II. Calculational Details

The calculations are similar to the calculations on Sc_3 which have been reported previously. The calculations use a relativistic effective core potential (ECP) developed by Hay and Wadt[3] which replaces the Ar core, but includes the 4s and 4p core levels in the calculation along with the 5s, 5p, and 4d valence electrons. The Y basis set is the same as the basis set reported by Hay and Wadt, except that the 5p functions are replaced by the functions recommended by Walch, Bauschlicher, and Nelin[4] multiplied by 1.5 to make them suitable for describing 5s $\rightarrow$5p correlation. The s and p basis sets are contracted (2111) based on the atomic 4s and 4p orbitals, respectively. The d basis set was contracted (211) and a single set of 4f functions was added as a two-term fit to a Slater orbital(ζ = 1.40)[4]. The basis set and ECP were tested by comparing ECP and all-electron calculations[7] for the $^5\Sigma_u^-$ state of the Y_2 molecule. The differences in the calculated potential curve parameters (ECP minus all-electron) were R_e= -0.01 a_0, ω_e= +4 cm^{-1}, and D_e= +0.04 eV.

The complete active space self consistent field (CASSCF) calculations[8] included the 5s-5p and 4d derived orbitals in the active space. For near equilateral triangle geometries the active orbitals were a_1' and e' from 5s, a_1' and e' from 4dσ, and a_2'' and e'' from 4dπ''. For linear geometries the active space included three σ_g, two σ_u, and one each π_{xu}, π_{xg}, π_{yu}, and π_{yg}. The nature of these orbitals is discussed in section III. As for the Sc_3 calculations[2], the number of electrons in symmetry subgroups was constrained to be the same as in the dominant configuration. For C_{2v} geometries, the symmetry subgroups were i) a_1 and b_2 and ii) a_2 and b_1, i.e. the orbitals were partitioned according to whether they were symmetric or asymmetric with respect to reflection in the molecular plane. For linear geometries, the symmetry subgroups were σ, π_x, and π_y. The CASSCF calculations were

followed by contracted configuration interaction (CCI) calculations[9]. Here the reference space included those configurations with coefficients greater than 0.1 in the CASSCF wavefunction near R_e (five, ten, and thirteen reference configurations for $^2A_1'$, $^2E'$, and $^2\Sigma_g^+$, respectively). This choice of reference configurations leads to valence CI energies within 0.1 eV of the CASSCF energy and reference percentages in the wavefunction of about 90 % . The calculations were carried out with the MOLECULE[5]- SWEDEN[6] system of programs.

III. Discussion

Table I summarizes the dominant configurations, geometries, symmetric stretch frequencies, T_e's, and Mulliken populations for the low-lying states of Sc_3 and Y_3. Tables II and III give CASSCF and CCI energies for equilateral triangle geometries for the $^2A_1'$, $^2A_2''$, and $^2E'$ states of Y_3.

The Sc_3 molecule has a $^2A_2''$ ground state with the configuration:

$4sa_1'^2\ 4se'^4\ 3da_1'^2\ 3da_2''^1$

and a very low-lying $^2A_1'$ state arising from the same limit with the configuration:

$4sa_1'^2\ 4se'^4\ 3da_1'^1\ 3da_2''^2$

Formally these configurations arise from three Sc atoms in the $4s^23d^1$ ground state. There is also a low-lying $^2E'$ excited state arising from two ground state Sc atoms and one Sc atom in the $4s^13d^2$ excited state:

$4sa_1'^2\ 4se'^3\ 3da_1'^2\ 3da_2''^2$

From Table I there are several obvious differences between Y_3 and Sc_3. The first difference is the larger p population for Y_3 as compared to Sc_3. Here Y_3 has a 5p population of 2.25 for the $^2A_1'$ ground state, while Sc_3 has a 4p population of 1.21 for the $^2A_1'$ state. For Sc_3 it was argued that the 4p population involved admixture of terms derived from the $4s^14p^13d^1$ Sc atomic configuration, which is at an excitation energy of 1.96 eV[10]. For Y atom the $5s^15p^14d^1$ configuration is at 1.91 eV[10];

thus, one would expect similar p populations if this were the only mechanism for mixing in p character. However, for the Y atom the lowest excited state has the configuration $5s^25p^1$ and is at an excitation energy of 1.33 eV[10]. By comparison, the analagous state for Sc atom is not observed experimentally, but is calculated to be at 3.06 eV from SCF calculations. Given the low-lying $5s^25p^1$ state of Y atom one expects that the ground state of Y_3 could arise from two atoms in the $5s^24d^1$ ground state and one atom in the low-lying $5s^25p^1$ state. States derived from this limit would still mix in $5s^15p^14d^1$ character leading to p populations about 1.0 greater than for states arising from three ground state atoms.

A second difference between Sc_3 and Y_3 is the different ordering of states. For Sc_3 the $^2A_1'$, $^2A_2''$, and $^2E'$ states are all close in energy; while, for Y_3 the ground state is $^2A_1'$ and the $^2A_1' \rightarrow {}^2A_2''$ excitation energy is 0.75 eV (from CASSCF calculations) for Y_3 as compared to -0.07 eV for Sc_3. This implies a stabilization of the $4da_2''$ orbital relative to the $4da_1'$ orbital for Y_3. The reason for this is obvious from the populations of the $4da_2''$ and $4da_1'$ orbitals. From Table IV. and Fig. 1 one sees a considerable admixture of 5p-4d character in the 4d bonding orbitals of Y_3, but much less admixture of 4p-3d character for Sc_3. This difference arises because of the more comparable 5p-4d orbital sizes as compared to the 4p-3d orbitals[7] and the smaller excitation energy to the $5s^25p^1$ state of Y atom as compared to the corresponding state of the Sc atom. Nonetheless, the 5p orbitals are still larger than the 4d orbitals so that distances corresponding to good 4d-4d overlaps[7] are well inside the optimal bonding radius for the 5p orbitals. Furthermore, the overlap integral $S_{5p\pi-5p\pi}$ increases monotonically toward one as R goes toward zero, but the overlap integral $S_{5p\sigma-5p\sigma}$ decreases inside the optimal bonding radius, eventually goes through zero, and becomes minus one for R equal zero. Thus, 4d-5p admixture is more favorable for $5p\pi$ than for $5p\sigma$ and this effect appears to be responsible for

the stabilization of the $4da_2''$ orbital relative to the $4da_1'$ orbital for Y_3.

We now consider non-equilateral triangle geometries. For C_{2v} symmetry the $^2A_1'$, $^2A_2''$, and $^2E'$ states correspond to $^2A_1$, $^2B_1$, and 2^2A_1 and $^2B_2$, respectively. Here the configurations are:

$^2A_1 = 1a_1^2 2a_1^2 1b_2^2 1b_1^2 3a_1^1$

$^2B_1 = 1a_1^2 2a_1^2 1b_2^2 1b_1^1 3a_1^2$

$2^2A_1 = 1a_1^2 2a_1^1 1b_2^2 1b_1^2 3a_1^2$

$^2B_2 = 1a_1^2 2a_1^2 1b_2^1 1b_1^2 3a_1^2$

We expect the $^2A_1'$ and $^2A_2''$ states to have equilateral triangle geometries, while the $^2E'$ state will Jahn-Teller distort leading to an acute angle minimum for the $^2B_2$ component and an obtuse angle minimum for the $^2A_1$ component. These expectations are confirmed by calculations. Table V gives CASSCF energies for the $^2A_1$ state of Y_3 for non-equilateral triangle geometries (with r_{Y-Y} fixed at 6.3 a_0 which is the optimal value for the $^2A_1'$ state from Table II.). Here one sees that the energy of the $^2A_1$ state goes up for obtuse angle geometries. Table V also shows energies for the 2^2A_1 state obtained as a second root of the CASSCF. Here one sees that, as expected, this state favors obtuse angle geometries.

For linear geometries, the 2^2A_1 configuration corresponds to:

$^2\Sigma_g^+ = 1\sigma_g^2 2\sigma_g^1 1\sigma_u^2 1\pi_{xu}^2 1\pi_{yu}^2$

Figure 2 shows key bonding orbitals for Y_3 for linear geometries. The $2\sigma_g$ orbital is basically a localized $4d\sigma$ orbital. The $1\pi_g$ orbital is a bonding orbital of primarily $4d\pi$ character, while the $1\pi_u$ orbital is of mixed character(mostly $5p\pi$ on the center atom and $4d\pi$ on the end atom). The occupations of these orbitals for the $^2\Sigma_g^+$ state are $2\sigma_g = 1.01$, $1\pi_u = 2$ x 1.11 and $1\pi_g = 2$ x 0.89. Given the very similiar populations for the $1\pi_u$ and $1\pi_g$ orbitals, this state is best thought of as an open shell doublet state derived from:

$^6\Sigma_g^+ = 1\sigma_g^2 2\sigma_g^1 1\sigma_u^2 1\pi_{xu}^1\ 1\pi_{xg}^1 1\pi_{yu}^1 1\pi_{yg}^1$

This change in the character of the wavefunction may be thought of in terms of a curve crossing between the 2^2A_1 configuration which is stable for near equilateral triangle geometries and the $^2\Sigma_g^+$ state which is stable for linear geometries. However, the $^2\Sigma_g^+$ state does retain some of the character of the $^2E'$ state as evidenced by the 4d population of 3.82.

Table VI gives CASSCF and CCI energies for the $^2\Sigma_g^+$ state of Y_3 for linear geometries. Table VII compares Mulliken populations for the $2\sigma_g$, $1\pi_{xu}$, and $1\pi_{xg}$ orbitals of the $^6\Sigma_g^+$ states of Y_3 and Sc_3, while plots of these orbitals are shown in Fig. 2. (The $^6\Sigma_g^+$ orbitals are found to be very similar to the $^2\Sigma_g^+$ orbitals for Y_3.) From Table VII and Fig. 2, one sees much more admixture of 5p and 4d in the π bonding orbitals of Y_3 as compared to the corresponding orbitals of Sc_3. This is particularly evident for the $1\pi_{xu}$ orbital. From Table VII it is seen that the latter orbital has about equal parts of 5p and 4d character for Y_3, but is mostly 4p like for Sc_3. These differences are also evident in the plots of these orbitals in Fig. 2. The $1\pi_{xu}$ orbital of Y_3 shows more 4d contours which is indicative of a Y(5pπ)-Y(4dπ) bond. The increased 5p-4d bonding in Y_3 is reflected in the small excitation energy to the $^6\Sigma_g^+$ state of 0.31 eV for Y_3 as compared to an excitation energy of 1.28 eV for the corresponding excitation in Sc_3(see Table I.).

The ESR spectrum of Y_3 is consistent with non equivalent Y atoms. The lowest state in the calculations is $^2A_1'$, which is expected to have an equilateral triangle geometry and is not consistent with the experiment (see Table V). It would be tempting to argue that the ground state of Y_3 is the linear $^2\Sigma_g^+$ state. This state is fully consistent with the ESR spectrum, since only parallel and perpendicular components of the g and A tensors were needed to simulate the spectrum. Also the singly occupied orbital has only about 5 % 5s character. The small amount of

5s character is consistent with the primarily 5p and 4d character of the $2\sigma_g$, $1\pi_{xu}$, $1\pi_{xg}$, $1\pi_{yu}$, and $1\pi_{yg}$ orbitals which are coupled together into a doublet spin state. The calculations do show that linear configurations are lower for Y_3 than for Sc_3, but the computed excitation energy of 1.54 eV is quite large.

It is not clear whether the computed excitation energy to the $^2\Sigma_g^+$ state could be off by more than 1.5 eV. We do note that for Ti_2 the ground state $^1\Sigma_g^+$ is computed to be 0.40 eV higher than the open shell $^7\Sigma_u^+$ state. Similarly, for Y_2, computations show a $^5\Sigma_u^-$ ground state, but ESR does not observe such a state and one possibility is that the true ground state is $^1\Sigma_g^+$, which is computed to be 0.87 eV higher. Thus, there is reason to believe that the calculations could have significant errors in the excitation energies for states of very different character. For the cases above we expect that the calculation will be biased toward open shell high-spin states over closed shell states. Similarly, for Y_3 the linear $^2\Sigma_g^+$ state has a much less compact zero order wavefunction than do the equilateral triangle states which are SCF dominated. Thus, one might also expect significant errors in the excitation energies here, and the ground state of Y_3 may be linear in agreement with one interpretation of the ESR spectrum of Y_3. Finally, we note that although the CCI calculations for the $^2\Sigma_g^+$ state correspond to more than one million configurations, the reference space is only about 90 % of the CI wavefunction. This problem, which has proven to be typical of calculations on transition metal dimers and trimers, is thought to arise because of the approximation of not including explicit nd shell correlation in the CASSCF wavefunction.

In spite of the difficulties in computing the excitation energies for these systems, these calculations show significant qualitative differences in the bonding in these molecules. This qualitative understanding of the bonding is important, since very little is known about the electronic structure of small transition metal clusters. Also

based on experience for transition metal diatomics [7], we expect that the computed geometries and force constants will be accurate and may provide some guidance to experimental studies on these molecules.

IV. Conclusions

We conclude that the bonding in Sc_3 and Y_3 differ mainly in terms of a larger p involvement in the bonding in Y_3 as compared to Sc_3. This larger p involvement arises because the $5s^25p^1$ state of the Y atom is low-lying(the first excited state), while the corresponding state for the Sc atom is at a large excitation energy. The result is that the lowest state of Y_3 for equilateral triangle geometries arises from two Y atoms in the $5s^24d^1$ state and one Y atom in the $5s^25p^1$ state, leading to a 5p population greater than two. For Sc_3, on the other hand, the lowest state arises from three ground state atoms and has a 4p population of about one.

In addition to the larger p population for Y_3, the 5p and 4d orbitals are more comparable in size than the 4p and 3d orbitals, which leads to significant 5p-4d hybridization in Y_3, but 4p-3d hybridization is not important in Sc_3. The 5p-4d hybridization stabilizes the $4da_2''(4d\pi'')$ orbital relative to the $4da_1'(4d\sigma)$ orbital. The latter effect leads to a $^2A_1'$ ground state for equilateral triangle Y_3, wheras, equilateral triangle Sc_3 has a $^2A_2''$ ground state.

For linear geometries Y_3 has a low-lying $^2\Sigma_g^+$ state. This state is much lower for Y_3 than for Sc_3 because of the formation of 5p-4d π bonds in Y_3. If this state were the ground state of Y_3 it would be fully consistent with the matrix ESR spectrum of Y_3. This assignment would require that the computed excitation energy to this state be in error by more than 1.5 eV. However, large errors in excitation energies for transition metal systems for states of different character have been observed for other systems, and thus the ground state of Y_3 may be linear in agreement with one possible interpretation of the ESR spectrum.

ACKNOWLEDGMENTS

S.P. Walch was supported by a NASA grant(NCC2-296).

References

1. L.B. Knight,Jr., R.W. Woodward, R.J. VanZee, and W. Weltner,Jr., J. Chem. Phys., **79**, 5820 (1983).
2. S.P. Walch and C.W. Bauschlicher,Jr., J. Chem. Phys., **83**, 5735(1985).
3. P.J. Hay and W.R. Wadt, J. Chem. Phys., **82**, 299(1985).
4. S.P. Walch, C.W. Bauschlicher,Jr., and C.J. Nelin, J. Chem. Phys., **79**, 3600(1983).
5. J. Almlöf, MOLECULE, a Gaussian integral program.
6. P.E.M. Siegbahn, C.W. Bauschlicher,Jr., B. Roos, A. Heiberg, P.R. Taylor, and J. Almlöf, SWEDEN, A vectorized SCF MCSCF direct CI.
7. S.P. Walch and C.W. Bauschlicher,Jr., Theoretical Studies of Transition Metal Dimers, in Comparison of Ab-Initio Quantum Chemistry with Experiment for Small Molecules, ed. by R.J. Bartlett (Reidel, 1985).
8. P.E.M. Siegbahn, A. Heiberg, B.O. Roos, and B. Levy, Physica Scripta, **21**, 323(1980).
9. P.E.M. Siegbahn, Int. J. Quantum Chem., **23**, 1869(1983).
10. C.E. Moore, Atomic Energy Levels, Natl. Bur. Stand. (U.S.) Circ. No. **467** (U.S. GPO, Washington, D.C., 1949)

Table I. Configurations, Potential Surface Parameters, and Mulliken Populations for Sc_3 [a] and Y_3.

		Potential Surface Parameters			Mulliken Populations			
State	Configuration	R_e[b],a_0	ω_e[c],cm^{-1}	T_e,eV	4s	4p	3d	4f
Sc_3 $^6\Sigma_g^+$	$1\sigma_g^2 1\sigma_u^2 2\sigma_g^1 1\pi_{xu}^1 1\pi_{xg}^1 1\pi_{yu}^1 1\pi_{yg}^1$			1.28[e]	2.67	2.11	4.18	0.04
Sc_3 $^2A_1'$	$4sa_1'^2 4se'^4 3da_1'^1 3da_2''^2$			0.07	4.50	1.21	3.25	0.04 [d]
Sc_3 $^2E'$	$4sa_1'^2 4se'^3 3da_1'^2 3da_2''^2$	5.61	204.	0.05	3.97	1.20	3.80	0.03
Sc_3 $^2A_2''$	$4sa_1'^2 4se'^4 3da_1'^2 3da_2''^1$	5.75	513.	0.00	4.61	1.11	3.25	0.03
					5s	5p	4d	4f
Y_3 $^2A_2''$	$5sa_1'^2 5se'^4 4da_1'^2 4da_2''^1$			0.75[e]				
Y_3 $^2E'$	$5sa_1'^2 5se'^3 4da_1'^2 4da_2''^2$	6.00	187.	0.46	2.94	2.21	3.76	0.09
Y_3 $^2\Sigma_g^+$	$1\sigma_g^2 1\sigma_u^2 2\sigma_g^1 1\pi_{xu}^1 1\pi_{xg}^1 1\pi_{yu}^1 1\pi_{yg}^1$	5.89		1.54	2.72	2.36	3.82	0.09
Y_3 $^6\Sigma_g^+$	$1\sigma_g^2 1\sigma_u^2 2\sigma_g^1 1\pi_{xu}^1 1\pi_{xg}^1 1\pi_{yu}^1 1\pi_{yg}^1$			0.31[e]	2.63	2.56	3.73	0.08
Y_3 $^2A_1'$	$5sa_1'^2 5se'^4 4da_1'^1 4da_2''^2$	6.32	264.	0.00	3.69	2.25	2.99	0.06

[a] Sc_3 results are from ref. 2.
[b] metal-metal distance.
[c] symmetric stretch frequency for D_{3h} geometry.
[d] R Sc-Sc = 5.5 a_0. The other populations are for the point closest to R_e
[e] CASSCF results

Table II. CASSCF Energies for Y_3 (Equilateral Triangle Geometries)

R(Y-Y)	$^2A_1'$	$^2E'$	$^2A_2''$
5.25		-112.37860	
5.50	-112.40823	-112.40455	
5.75		-112.41844	
6.00	-112.44621	-112.42295	-112.41858
6.30	-112.45092	-112.41944	
6.50	-112.44918		
7.00	-112.43454		

Table III. CCI Energies for Y_3 (Equilateral Triangle Geometries)

R(Y-Y)	$^2A_1'$	$^2E'$
5.50		-112.56399
5.75		-112.57800
6.00	-112.5[illegible]0	-112.58221
6.30	-112.59[illegible]7	-112.57768
6.50	-112.59524	
7.00	-112.57640	

Table IV. Mulliken Populations for Selected Orbitals for Sc_3 and Y_3 for the $^2A_1'$ state.

	s	p	d	f
$Sc_3(3da_1')$	0.01679	0.07461	0.73747	0.01106
$Y_3(4da_1')$	0.03922	0.23463	0.71649	0.02088
$Sc_3(3da_2'')$	0.00000	0.18008	1.39599	0.01473
$Y_3(4da_2'')$	0.00000	0.48791	1.34106	0.01985

Table V. CASSCF Energies for Y_3 (Non-Equilateral Triangle Geometries)

R(Y-Y)	θ	$^2A_1$	2^2A_1
6.30	60.	-112.45092	-112.39422
6.30	75.	-112.43708	-112.40411
6.30	90.	-112.41910	-112.39700
6.30	120.	-112.3985	-112.3734

Table VI. CASSCF and CCI Energies for Y_3 (Linear Geometries)

R(Y-Y)	CASSCF	CCI
5.50	-112.41611	-112.53973
5.75	-112.42374	-112.54227
6.00	-112.42587	-112.54239
6.30	-112.42279	-112.54006

Table VII. Mulliken Populations for Selected Orbitals for Sc_3 and Y_3 for the $^6\Sigma^+$ state.

	s	p	d	f
$Sc_3(2\sigma_g)$	0.03671	0.00218	0.98366	0.00001
$Y_3(2\sigma_g)$	0.25686	0.06009	0.67001	0.00437
$Sc_3(1\pi_{xu})$	0.00000	0.81349	0.17874	0.00868
$Y_3(1\pi_{xu})$	0.00000	0.45445	0.52200	0.02225
$Sc_3(1\pi_{xg})$	0.00000	0.10594	0.88688	0.00631
$Y_3(1\pi_{xg})$	0.00000	0.13547	0.85645	0.00938

Figure Captions.

Figure 1. Contour plots of selected orbitals of the $^2A_2''$ state of Sc_3 and the $^2A_1'$ state of Y_3 for equilateral triangle geometries. The orbitals are plotted in a plane perpendicular to the molecular plane and passing through one atom and the center of the opposite bond. Positive contours are denoted by solid lines, negative contours are denoted by dotted lines, and nodal surfaces are denoted by dashed lines.

Figure 2. Contour plots of selected orbitals for the $^6\Sigma_g^+$ state of Sc_3 and Y_3 for linear geometries. The orbitals are plotted in the molecular plane. The conventions are the same as in Fig. 1.

Fig. 1

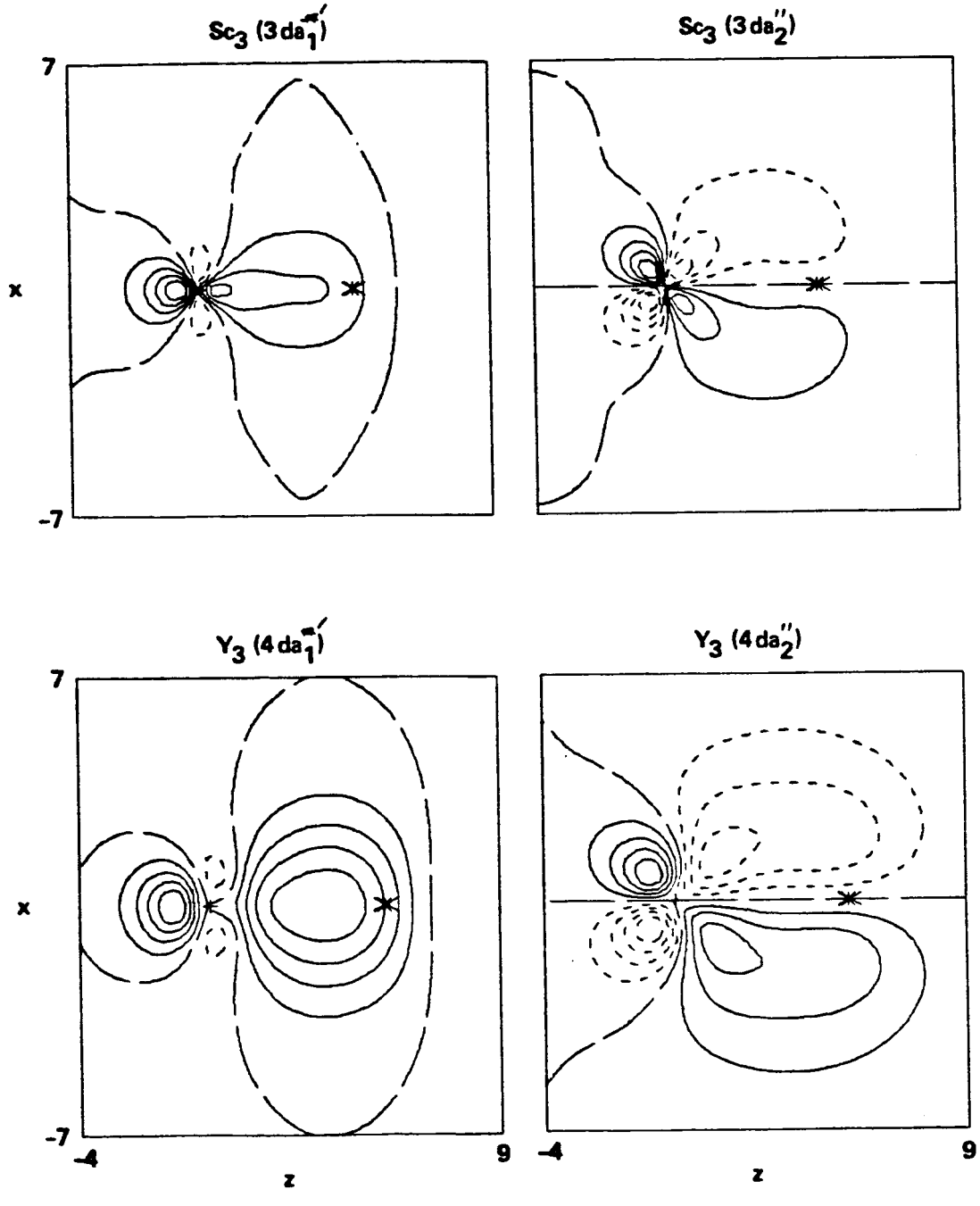

Fig. 2